Available online at www.sciencedirect.com
SCIENCE DIRECT®

Journal of the European Ceramic Society 23 (2003) 2955–2962
www.elsevier.com/locate/jeurceramsoc

Microstructure, mechanical properties and stability of nitrided Y-TZP

A. Feder, J. Alcalá, L. Llanes, M. Anglada*

Department of Materials Science and Metallurgy, Universitat Politècnica de Catalunya, ETSEIB, Avda. Diagonal 647, 08028 Barcelona, Spain

Abstract

The mechanical properties and microstructure of nitrided tetragonal zirconia polycrystals doped with yttria (Y-TZP) have been evaluated. It has been established that a surface layer is formed during nitriding at 1650 °C for 5 min, 1 and 2 h. Such layer exhibits a gradient in grain size, which results in a variation in the capacity of the material to undergo a stress assisted tetragonal to monoclinic (t–m) phase transformation together with a build up of residual stresses. After nitriding for 1 h, the outer surface forms non-transformable t′ phase, which protects the material from low temperature ageing degradation. It is shown that, in contrast with the original Y-TZP, the nitrided surface does not transform in the presence of water at 100 °C during time periods of up to 900 h. By contrast, nitrided Y-TZP is not stable after exposure in air at temperatures of 600 and 800 °C, since t–m transformation occurs in a subsurface layer of the nitrided rods, and this induces high internal stresses.

Keywords: Diffusion; Grain size; Hardness; Interfaces; Nitridation

1. Introduction

The stability of ZrO_2 polymorphs depends strongly upon the quantity and type of stabilising oxide that is used to decrease the temperature of the tetragonal to monoclinic (t–m) phase transformation. This transformation is martensitic in nature and is accompanied by an increase in volume of up to approximately 4%. In the event that such transformation becomes active under a stress field in the vicinity of a crack, a slight change in volume occurs ahead of the crack tip, leading to a significant increase in the fracture toughness.[1] Unfortunately, this transformation may also take place at the surface due to interaction with water molecules in the environment. Such interaction induces surface cracks which, in turn, results in a degradation of the mechanical properties (see, for instance, Ref. 2).

One strategy to increase the resistance of Y-TZP against humidity is to act upon the microstructure of the material at the surface exposed to the environment. This can be accomplished by various methods, such as crystallisation of tetragonal grains in the surface region,[3] sintering green Y-TZP compacts in a powder bed of stabilising oxides such as Y_2O_3,[4] or by doping with silica.[5] Along these lines, a method that deserves to be explored involves surface nitriding.[6] The operating mechanism behind this approach is the formation of vacancies in the unit-cell of zirconia which are induced by a high-temperature heat treatment in the presence of nitrogen. This element stabilises the cubic phase of zirconia (c-ZrO_2) by virtue of a partial substitution of oxygen ions (O^{2-}) by nitrogen ions (N^{3-}), causing the desired vacancies.[7] This mechanism is identical to that of bi and tri-valent cations, such as Mg^{2+} and Y^{3+}, which allows stabilising the tetragonal and cubic phases of ZrO_2.

In this work, it is investigated the microstructure, mechanical properties and stability of nitrided Y-TZP. It is shown that the nitrided material does not suffer hydrothermal degradation after exposure at 100 °C for long times, but t–m transformation is detected in a subsurface layer after exposing the nitrided material at 600 and 800 °C in air.

2. Experimental procedure

The starting material examined in this work is a zirconia stabilised with 2.5% mol of Y_2O_3 (Y-TZP). Its microstructure consists of tetragonal grains with an

* Corresponding author. Tel.: +34-93-4016-707; fax: +34-93-4016-706.
E-mail address: marc.j.anglada@upc.es (M. Anglada).

0955-2219/03/$ - see front matter © 2003 Elsevier Ltd. All rights reserved.
doi:10.1016/S0955-2219(03)00307-8

average size of 0.3 μm. The specimens had the shape of cylindrical bars of 8 mm in diameter. They were initially covered with a fine-grain powder of ZrN (having a maximum particle size of 7.7 μm) and then heat treated in a nitrogen-rich environment at a temperature of 1650 °C during 5 min, 1 and 2 h. The resulting materials are referred to as 5M, 1H and 2H, respectively. The heating and cooling rates applied were both of 20 °C/min. Some transversal slices of the rods were also nitrided, for the 5M and 2H conditions, in order to prepare thin foils for transmission electron microscopy (TEM) of the surface region.

The nitrided rods were also cut in disks of about 2 mm thickness and polished using diamond pastes until a mirror finish was attained. To reveal the microstructure, thin slices of 30 μm thickness were analysed by transmission optical microscopy (TOM).

Microhardness tests with a 0.98 N load were conducted to evaluate the variation in hardness along the diameter of the rods. In addition, Vickers indentation tests were carried out to induce cracks at various distances from the surface with the objective of studying the fracture behaviour of the nitrided materials. In prior work, it has been shown that the geometry of cracks introduced by Vickers indentation in Y-TZP exhibits a Palmqvist-type shape.[8] However, since the microstructure of nitrided Y-TZP changes with distance to the surface of the specimens, the shape of the indentation cracks at different positions inside the rod may be different. Therefore, the fracture toughness K_{Ic} was evaluated using the equation derived by Anstis et al.[9] which has also been widely used in Y-TZP for either Palmqvist or radial cracks,[10]

$$K_{Ic} = \chi \frac{P}{c_0^{3/2}} \quad (1)$$

where χ is a factor that depends on both Young's modulus E and hardness H, P is the applied indentation load, and $2c_0$ is the average length of the induced cracks.

Experiments of hydrothermal degradation were carried out with the purpose of evaluating the influence of water on microstructural stability of the nitrided specimens. Such experiments were performed by submerging the polished and nitrided Y-TZP disks in water at 100 °C during different periods of time. The t–m transformation at the surface was analysed by Raman microprobe spectroscopy.

It is known that *nitrided* Y-TZP may suffer a spontaneous transformation to monoclinic phase when heat treated in air at temperatures higher than 600 °C.[6] For this reason, the stability of the phases in the nitrided rods was studied in air at temperatures of 600 and 800 °C for time intervals of 1, 2, 4 and 8 h by using disks sliced from the rods and carefully polished with 30 and 6 μm diamond pastes. The aim of these experiments was to analyse the influence of oxygen on the coarse tetragonal phase induced by nitrogen after nitriding. The microstructural evolution resulting from such treatments in air was assessed through Raman microprobe spectroscopy. The fraction of monoclinic phase present in different regions of the specimens was calculated using an equation attained from calibration using X-ray data, as reported in a previous work by the authors.[11]

3. Results and discussion

3.1. Microstructural characterisation of nitrided Y-TZP

Fig. 1 shows the microstructure of Y-TZP after nitriding at 1650 °C for 2 h. A surface layer is formed in the nitrided samples with a thickness that increases with nitriding time. Two regions can be discerned in the nitrided layer according to the grain size (see Table 1): Region I, which is the outermost zone of the specimens, and it contains a microstructure with a large homogeneous grain size, and its thickness is approximately 350 μm for 2H, and ~250 μm for 1H; Region II, which extends to the interface between the above layer and the bulk and exhibits a gradient in grain size from 4 to 1 μm for the three nitriding times used here. The material in the bulk (denoted as Region III) exhibits a homogeneous microstructure whose grain size is also included in Table 1. Raman analysis indicated that there is no monoclinic phase in the nitrided materials. TEM analysis of the outermost region (zone I) of 5M and 2H reveal that the morphology of the microstructure depends on nitriding time. For the case of 5M, a heterogeneous distribution of fine precipitates is detected (Fig. 2a). On the other hand, in 2H the surface grains have a domain structure that is typical of non-transformable (t′) phase.[12] These domains have a nanometric thickness

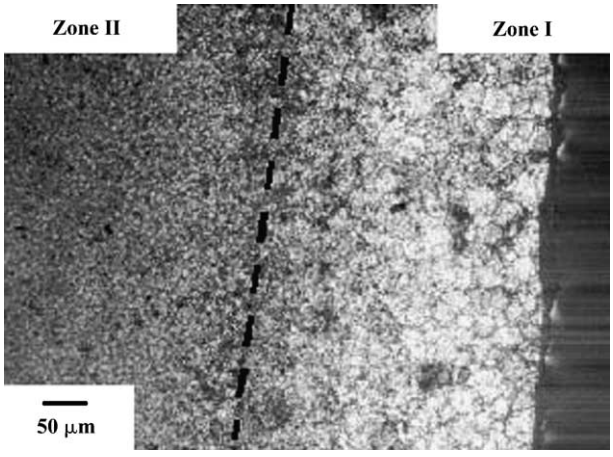

Fig. 1. TOM micrograph of Y-TZP nitrided during 2 h at 1650 °C (2H).

and exhibit three orientations as shown in Fig. 2b. The above microstructural differences are mostly associated with the time selected for nitriding. Thus, after nitriding for only 5 min, precipitates are present in the interior of the cubic grains at the surface, but the tetragonal domains develop only after longer nitriding times (2 h). The reason may be that the c-phase is stabilised at the surface at high temperature due to the presence of a large amount of nitrogen, but it transforms to (t′) upon cooling to room temperature.[13] This transformation is accompanied by the formation of the tetragonal domains shown in Fig. 2b. These findings are in good concordance with the results by Cheng and Thompson that show a decrease in the t–c transformation temperature as ZrN is added into Y-TZP.[13]

3.2. Mechanical characterisation

As described above, the nitriding process leads to the formation of a surface layer with different microstructures. Thus, one would also expect that the mechanical properties will depend on the region of the layer where they are measured. The variation of microhardness with depth for indentation loads of 0.98 N is shown in Fig. 3. The microhardness (H_v) in the surface region of 1H and 2H is larger than for the original Y-TZP.

Table 1
Depth of nitrided layers formed as a function of nitriding time and corresponding grain size values

Material	5M	1H	2H
Depth of zone I (μm)	~25	~250	~350
Mean grain size in zone I (μm)	~8	~15	~20
Depth of zone II (μm)	~100	~450	~850
Mean grain size in zone III (μm)	~0.3	~0.8	~1.1

The value of H_v in Region I of 1H is ~14.5 GPa and it decreases gradually as the depth increases until reaching values similar to those of the original material (~12 GPa). Hence, the increase in hardness in the surface layers could be related to (1) a larger concentration of nitrogen present in such regions, (2) a larger grain size, and (3) the presence of t′-phase. In the case of 5M, the hardness is not found to vary, within the experimental scatter. This result may also be explained by the presence of some cubic phase which is generally softer than the t′-phase. In addition, it should be noticed that the hardness at the surface for 2H is smaller than for 1H. This could be related to an increase in the size of tetragonal (t′) domains as observed by TEM in specimens nitrided for 1 and 2 h.

The variation of K_{Ic} at the centre of the nitrided rods and in the original material is presented in Fig. 4. The increase in fracture toughness measured at the centre of

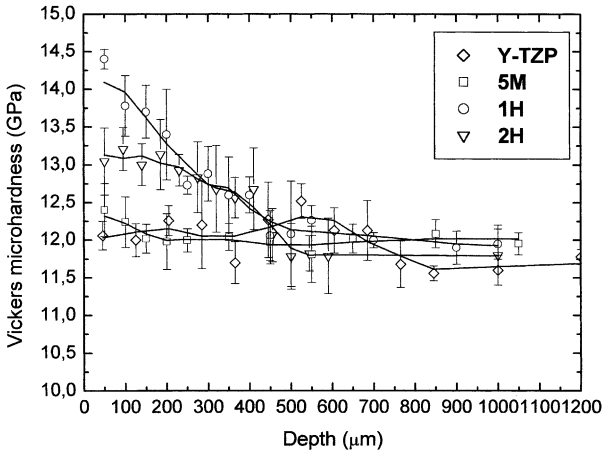

Fig. 3. Vickers microhardness profiles as a function of depth for 5M, 1H, 2H, and starting Y-TZP.

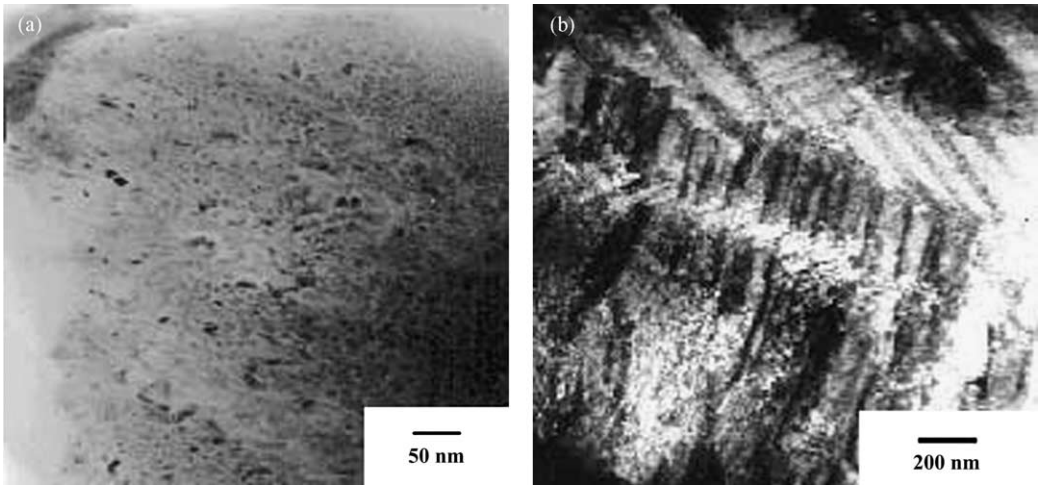

Fig. 2. TEM micrographs of zone I of nitrided Y-TZP: (a) 5M (5 min), (b) 2H (2 h).

nitrided rods with respect to the starting Y-TZP is associated with differences in grain size. Since the tetragonal grain size increases in the nitrided specimens (see Table 1), the energy to activate the t–m phase transformation under applied stresses decreases, resulting in an enhancement in fracture toughness. This interpretation is also substantiated by the observation that when the grain size is increased by heat treating the rods in air at 1650 °C for the same time, the fracture toughness also increase and reach similar values to those measured here at the centre of specimens nitrided at the same temperature.[8]

The Vickers indentation technique was also used to study the length of the cracks at different depths (Fig. 5a). It has been found that, in the nitrided layer, crack lengths in the radial direction are clearly different from those in the tangential one. This implies the existence of residual stresses which should be compressive in the tangential direction and tensile in the radial one (see Fig. 5b). The difference in crack lengths between both directions increases with nitriding time.

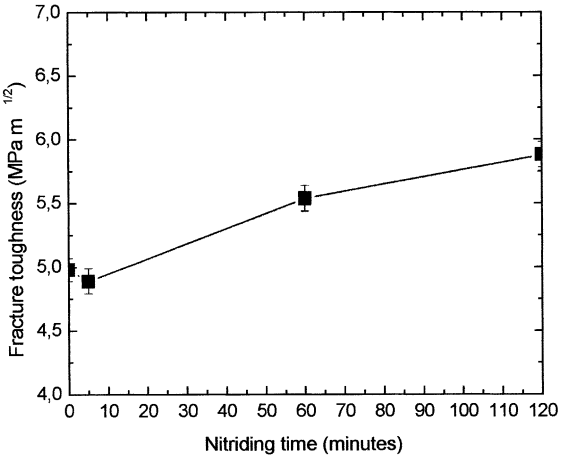

Fig. 4. K_{Ic} as a function of nitriding time at the centre of the bars (zone III).

Attempting to rationalise the existence of residual stresses, the transformations that take place during nitriding as well as the nitrogen concentration gradient along the radial direction should be analysed. As the chemical concentration gradient may cause a lattice dilation, a stress distribution may arise inside the nitrided rod which can be calculated by using solutions obtained for the stresses caused by thermal gradients and that have been applied to diffusion problems accompanied by change in volume.[14] Hence, the stress field that results is compressive in the tangential direction and decreases with depth, while the radial component is tensile, and near the surface increases slowly with depth. In this sense, it should be recalled that nitrogen in Y-TZP forms nitrogen ions (N^{3-}) which substitute oxygen ones (O^{2-}).[7] Such introduction of ions with larger ionic radii may result in a residual stress build up during nitriding if these are not relaxed by the production of enough oxygen vacancies.

In order to quantify the residual stresses present in the nitrided layer, we shall assume that the indentation crack is subjected to a constant radial and tangential residual stress field. As it has been proposed by Zeng and Rowcliffe,[15] for calculating this residual stress field it is necessary to have a prior knowledge of the length of indentation cracks (c_0) in a fresh (stress-free) specimen as well as in the surface where the residual stresses are to be evaluated. To apply this model to the case at hand, let us start by assuming that Region III is stress-free because the crack lengths in the different materials are similar within this zone. Thus, considering that the fracture toughness in a stress-free surface is given by Eq. (1), in the event that residual stresses are present at the indented surface, the apparent fracture toughness (K_{ap}) may be written as

$$K_{ap} = K^{*}_{Ic} - K_{res} \quad (2)$$

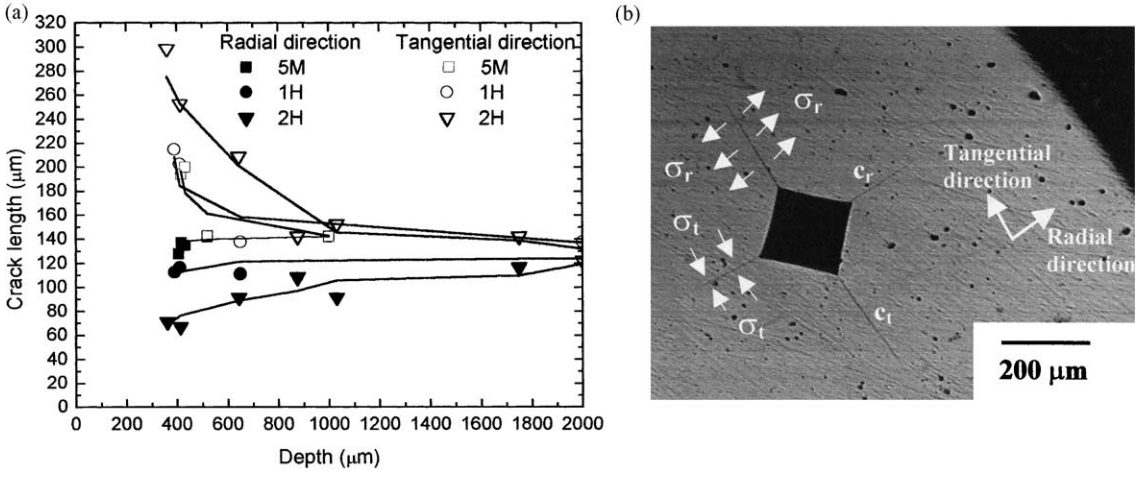

Fig. 5. (a) Crack lengths, for an indentation load of 294 N, as a function of sample depth; (b) indentation near the surface in 2H.

where K^*_{Ic} is the fracture toughness at the point of indentation and K_{res} is the stress intensity factor due to internal stresses (K_{res} is taken as positive for tension and negative for compression). If Eq. (2) is applied to the indentation cracks in the radial, $K_{res} = K_r$, and tangential directions, $K_{res} = K_t$, we obtain:

$$\frac{\chi P}{c_r^{3/2}} = K^*_{Ic} - K_r \tag{3}$$

$$\frac{\chi P}{c_t^{3/2}} = K^*_{Ic} - K_t \tag{4}$$

where $2c_r$ and $2c_t$ are the crack lengths in the radial and tangential directions, respectively (see Fig. 5b). Then, by subtracting both equations and dividing by the fracture toughness in the centre of the rods, K_{Ic}, which is supposed to be stress free, it is possible to obtain the difference between the internal stress intensity factors in the radial and tangential directions, that is,

$$\frac{K_t - K_r}{K_{Ic}} = c_0^{3/2}\left(\frac{1}{c_t^{3/2}} - \frac{1}{c_r^{3/2}}\right) \tag{5}$$

where $2c_0$ is the crack length at the centre of the rod. This variation is plotted in terms of the distance to the surface in Fig. 6. It can be noticed that $(K_t - K_r)/K_{Ic}$ decreases from the centre to the surface and it reaches a value of the order of 1 near the outer t′ layer. This means that the average of absolute values of the stress intensity factors induced by internal stresses may reach values close to the fracture toughness.

If the expressions for the stress intensity factors for surface semicircular cracks under a constant stress are used, the stress intensity factors of the internal stresses can be written as,

$$K_r = \phi\sigma_t\sqrt{c_r} \tag{6}$$

$$K_t = \phi\sigma_r\sqrt{c_t} \tag{7}$$

where ϕ is a constant of the order to unity and σ_r and σ_t are the radial and tangential internal stresses, which act in mode I, that is perpendicular to the tangential and radial indentation cracks, respectively. From Eqs. (3) and (4), and by using Eqs. (6) and (7), we have

$$\sigma_r = K_{Ic}\frac{\left[(c_0/c_t)^{3/2} - \left(K^*_{Ic}/K_{Ic}\right)\right]}{\phi c_t^{1/2}} \tag{8}$$

$$\sigma_t = K_{Ic}\frac{\left[(c_0/c_r)^{3/2} - \left(K^*_{Ic}/K_{Ic}\right)\right]}{\phi c_r^{1/2}} \tag{9}$$

To estimate the residual stress, it is necessary to know the local fracture toughness along the radial direction of the rod. This parameter is not constant since the microstructure changes along this direction, with large tetragonal grains in Region II, close to the t′ outer layer and fine grains at the centre of the rod. Then, only a rough estimation can be given by neglecting these changes and taking $K_{Ic} = K^*_{Ic}$. By doing so, the internal stresses along both directions can be estimated by measuring the crack lengths at different depths and the results are shown in Fig. 7. It is clear that these values are only a first approximation to the residual stresses. Indeed, since the nitrided material below the t′-layer is more transformable, indentation crack lengths are different from those at the centre of the rod, not only because of the existence of residual stresses, but also because at this place the material has a higher fracture toughness. However, since an increase in K_{Ic} should have the same effect for the radial and tangential directions, the asymmetric behaviour is entirely due to the internal stresses developed inside the rod. If, as expected, the local fracture toughness was generally higher than at the centre of the rod, the present estimations would tend to overestimate the tensile internal stress

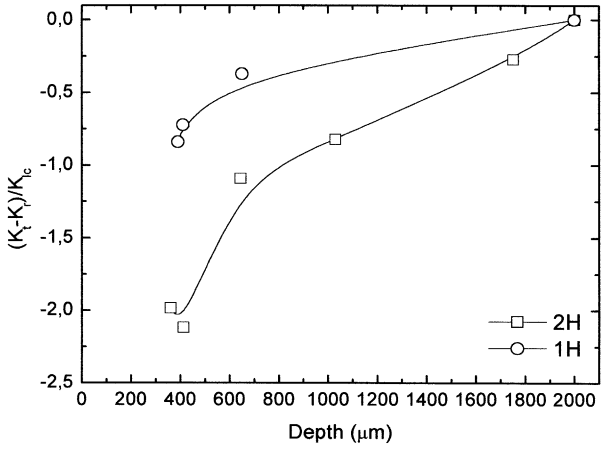

Fig. 6. Variation of $(K_t - K_r)/K_{Ic}$ as a function of sample depth.

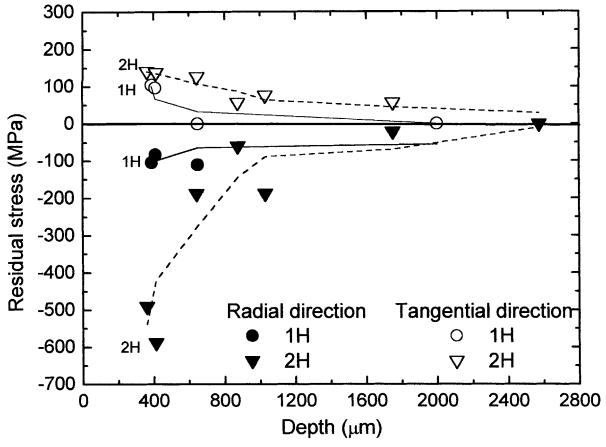

Fig. 7. Residual stresses, calculated using Eq. (7), as a function of sample depth for 1H and 2H.

and to subestimate the compressive ones. Then, the values measured for the compressive internal stresses at different points should be taken as a lower bound to the exact value.

3.3. Hydrothermal degradation

It is well known that transformation of the t-phase to monoclinic at the surface of Y-TZP is facilitated by the presence of humidity at temperatures up to 300 °C.[2] In the present work, the resistance against hydrothermal-induced phase transformation of nitrided specimens has been studied and compared to the results obtained for Y-TZP under similar conditions. The fraction of m-phase induced at the surface of disks subjected to hydrothermal degradation at 100 °C is presented in Fig. 8 as a function of time. It is clearly seen that for the original Y-TZP the fraction of m-phase detected by Raman spectroscopy increases with ageing time, whereas no m-phase has been found at the surface of the nitrided 2H disks after similar hydrothermal exposure. This finding indicates the non-transformable character of the microstructure at Y-TZP nitrided surfaces.

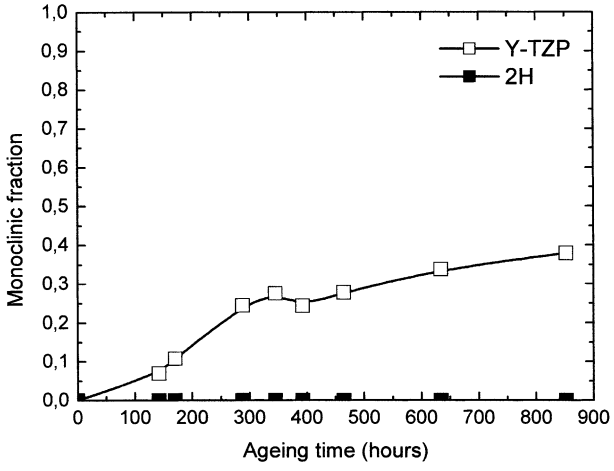

Fig. 8. Volume fraction of monoclinic phase at the surface in terms of ageing time in water at 100 °C.

3.4. Microstructural characterisation of nitrided Y-TZP after heat treating at 600 and 800 °C in air

Heat treatments at 600 and 800 °C of nitrided Y-TZP specimens were conducted in air in order to study the stability of the phases within the surface layer of materials 5M, 1H and 2H. These temperatures were selected in order to see if at these low temperatures diffusion of oxygen and nitrogen in the nitrided specimens could affect the stability of the tetragonal phase. Particularly, this could be relevant in regions with a large tetragonal grain size as it occurs underneath the t′ external layer. Because of the well known relationship between stability of the tetragonal grain size and number of vacancies, this place is where a higher volume fraction of oxygen vacancies should be present. Since it is also the place where the tetragonal phase is closer to the surface, it is expected that oxygen diffusion at high temperature could decrease the number of vacancies and activate the t–m phase transformation.

It is noted that Region I should be highly stable at such temperatures because of the presence of non-transformable t′ and c phases. Fig. 9 shows the fraction of monoclinic phase in terms of depth, heat treatment, temperature and time. It is found that in specimens 1H and 2H, the fraction of monoclinic phase reaches a maximum of about 0.6, which is essentially independent of time and temperature, while for 5M such maximum is only about 0.4.

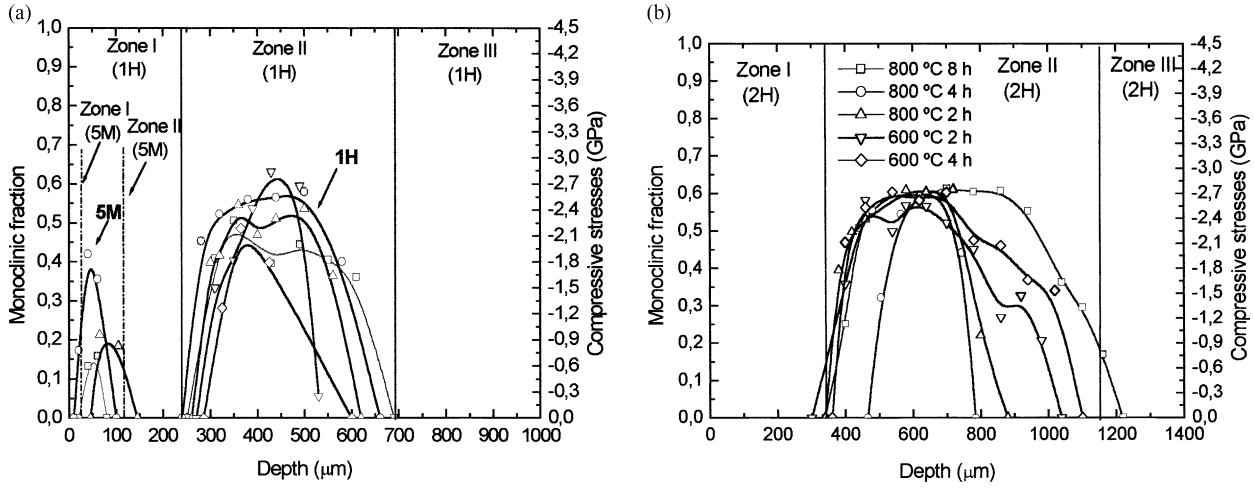

Fig. 9. Variation of fraction of monoclinic phase and corresponding residual compressive stresses for: (a) 5M and 1H, (b) 2H.

As the t–m transformation is accompanied by an increase in volume ($\Delta V/V$), the residual stresses introduced at each point may be related to the fraction of monoclinic phase by means of the following expression[14]

$$\sigma_c \approx \frac{1}{3}\left(\frac{\Delta V}{V}\right)\frac{EV_i}{(1-\nu)} \quad (10)$$

and the correspondingly attained values are also shown at the right hand axis of Fig. 9.

From Fig. 9 it is readily discerned that Region I does not undergo any transformation because the fraction of m-phase is zero. Note that thickness of the protective layer for material 2H (~350 μm) is about $\sqrt{2}$ times that of the stable layer in material 1H (~250 μm) as it could be anticipated from the laws governing a diffusional process. Accordingly, this means that t′-phase appears when a critical nitrogen concentration is reached. The depth at which the fraction of monoclinic is again zero (~1200 μm in 2H and ~680 μm in 1H) satisfactorily coincides with the location were Region III begins. The protective layer for 5M (~25 μm) is much thinner than in the other cases because the nitriding time is also shorter, and this leads to a reduction in the amount of nitrogen introduced into the material.

The cause for the non-transformability of the t′-phase in the outer layer in 1H and 2H, despite of its large grain size, has been explained by the idea that the resistance to experience t–m transformation is controlled by the size of the tetragonal domains.[16] In our case, these domains are extremely thin as their thickness is about 50 nm (see Fig. 2b). Furthermore, the transformability of the tetragonal phase in Region II at temperatures of 600 and 800 °C is anticipated to depend on various factors such as: (1) nitrogen content dissolved during nitriding at 1650 °C, (2) fraction and grain size of the tetragonal phase, and (3) existence of non-transformable phases.

The distribution of the m-phase in Region II may be analysed by considering that at the border with Region I, there is a continuous transition from only t′-phase to c-and t-phase. The nitrogen content is still high so that the non-transformable c- and t′-phases are still stable and, thus, the loss in nitrogen does not induce transformation. Near the border is even possible to observe grains of 4 μm, which cannot be tetragonal because they are larger than the critical size for spontaneous transformation to m-ZrO_2. Near the centre of Region II, t-phase becomes predominant as it is shown by the increase in the fraction of m-phase at the centre of Region II. This is the consequence of the transformation of the t-phase when the amount of stabiliser (nitrogen/oxygen vacancies) in this phase is decreased during high temperature exposure. After the maximum amount of transformation is reached, a significant decrease in the fraction of m-phase is detected which could be related to the fact that the grain size of the t-phase in this region is smaller and, thus, its transformability is also reduced.

Finally, the absence of monoclinic phase in Region III can be explained by a lower concentration of nitrogen, so that a negligible amount of stabiliser is lost during the heat treating in air. In addition, the grain size is relatively small, which makes the tetragonal phase more stable in front of the t–m transformation.

3.5. Mechanical characteristics of nitrided bars after exposed to 600 and 800 °C in air

The heat treatments in air induce the t–m transformation underneath the nitrided (surface) layer. From the knowledge of the fraction of m-phase, it is possible to estimate the level of the compressive stresses resulting from the increase in volume that accompanies the above phase transformation according to Eq. (10). Fig. 9 indicates that maximum values of σ_c attained in nitrided disks are about −2.7 GPa for a monoclinic volume fraction of ~0.6. According to this high compressive stress level, indentation cracks should be shorter than the crack length for which Eq. (1) is valid. Experimental confirmation for this has been obtained by indenting Region II with a load of 294 N and observing that no cracks are induced at the corners of the imprint when this region has transformed. On the contrary, indentation cracks in Region III become longer and finally their lengths are similar to those at the centre of the rods. Additionally, the values of K_{Ic} in such region are only slightly larger than those of non-nitrided specimens heat treated during 2 h at 1650 °C in air (Fig. 4).

4. Conclusions

A protective layer that is resistant to water degradation has been introduced in a Y-TZP ceramic stabilised by 2.5 mol% of Y_2O_3. This has been achieved by recourse to suitable nitriding heat treatments of the original material. The nitrided layer is formed by non-transformable t′-phase, which does not transform to monoclinic by interaction with the water in the environment.

The tetragonal t-phase of nitrided Y-TZP, which is capable of transforming to the monoclinic structure, remains in the interior of the specimens. However, at temperatures of 600 and 800 °C in air, a subsurface tetragonal layer transforms inducing large residual stresses.

Acknowledgements

The authors wish to thank the Ministry of Science and Technology of Spain for funding this investigation

through grant MAT-99-0781. Financial support provided by Generalitat de Catalunya with grant 2001SGR00229 is also acknowledged.

References

1. McMeeking, R. and Evans, A. G., Mechanics of transformation toughening in brittle materials. *J. Am. Ceram. Soc.*, 1982, **65**, 242–246.
2. Sato, T., Ohtaki, S., Endo, T. and Shimada, M., Changes in crystalline phase and microstructure on the surface of yttria-doped tetragonal zirconia polycrystals (Y-TZP) by annealing in humid conditions. *Advances in Ceramics Vol. 24: Science and Technology of Zirconia III*, 1988, 501–508.
3. Whalen, P. J., Reidinger, F. and Antrim, R. F., Prevention of low-temperature surface transformation by surface recrystalization in yttria-doped tetragonal zirconia. *J. Am. Ceram. Soc.*, 1989, **72**, 319–321.
4. Schubert, H., Claussen, N. and Rühle, M., Surface stabilization of Y-TZP. *Proc. Br. Ceram. Soc.*, 1984, **34**, 157–160.
5. Gremillard, L., Epicier, T., Chevalier, J. and Fantozzi, G., Microstructural study of silica-doped zirconia ceramics. *Acta Mater.*, 2000, **48**, 4647–4652.
6. Chung, T. J., Song, H., Kim, G. H. and Kim, D. Y., Microstructure and phase stability of yttria-doped tetragonal zirconia polycrystals heat treated in nitrogen atmosphere. *J. Am. Ceram. Soc.*, 1997, **80**, 2607–2612.
7. Claussen, N., Wagner, R., Gauckler, L. J. and Petzow, G., Nitride-stabilized cubic zirconia. *J. Am. Ceram. Soc.*, 1978, **61**, 369–370.
8. Casellas, D., Feder, A., Llanes, L. and Anglada, M., Fracture toughness and mechanical strength of Y-TZP/PSZ ceramics. *Scripta Mater.*, 2001, **45**, 213–220.
9. Anstis, G. R., Chantikul, P., Lawn, B. R. and Marshall, D. B., A critical evaluation of indentation techniques for measuring fracture toughness: I, direct crack measurements. *J. Am. Ceram. Soc.*, 1981, **64**, 533–538.
10. Kaliszewski, M. S., Behrens, G., Heuer, A. H., Shaw, M. C., Marshall, D. B., Dransmann, G. W., Steinbrech, R. W., Pajares, A., Guiberteau, F., Cumbrera, F. L. and Dominguez-Rodriguez, A., Indentation studies on Y_2O_3-stabilized ZrO_2: I, Development of indentation-induced cracks. *J. Am. Ceram. Soc.*, 1994, **77**, 1185–1193.
11. Casellas, D., Cumbrera, F. L., Sánchez-Bajo, F., Forsling, W., Llanes, L. and Anglada, M., On the transformation toughening of Y-ZrO_2 ceramics with mixed Y-TZP/PSZ microstructures. *J. Eur. Ceram. Soc.*, 2001, **21**, 765–777.
12. Sakuma, T., Microstructural aspects on the cubic-tetragonal transformation in zirconia. *Key Engng. Mat.*, 1998, **153-154**, 75–96.
13. Cheng, Y.-B. and Thompson, D. P., Role of anion vacancies in nitrogen-stabilized zirconia. *J. Am. Ceram. Soc.*, 1993, **76**, 683–688.
14. Richmond, O., Leslie, W. C. and Wriedt, H. A., Theory of residual stresses due to chemical concentration gradients. *A.S.M. Trans. Q*, 1964, **57**, 294–300.
15. Zeng, K. and Rowcliffe, D., Experimental measurement of residual stress field around a sharp indentation in glass. *J. Am. Ceram. Soc.*, 1994, **77**, 524–530.
16. Jue, J. F., Chen, J. and Virkar, A., Low-temperature aging of t′-zirconia: the role of microstructure on phase stability. *J. Am. Ceram. Soc.*, 1991, **74**, 1811–1820.